

Article

Not peer-reviewed version

Optical and Electronic Expert System for Diagnosing Eye Pathology in Glaucoma

[Orken Mamyrbayev](#) , [Sergii Pavlov](#) , Yosip Saldan , [Kymbat Momynzhanova](#) ^{*} , [Sholpan Zhumagulova](#)

Posted Date: 12 July 2024

doi: 10.20944/preprints2024071038.v1

Keywords: optical and electronic expert system; diagnosing eye pathology; glaucoma




Preprints.org is a free multidiscipline platform providing preprint service that is dedicated to making early versions of research outputs permanently available and citable. Preprints posted at Preprints.org appear in Web of Science, Crossref, Google Scholar, Scilit, Europe PMC.

Copyright: This is an open access article distributed under the Creative Commons Attribution License which permits unrestricted use, distribution, and reproduction in any medium, provided the original work is properly cited.

Article

Optical and Electronic Expert System for Diagnosing Eye Pathology in Glaucoma

Orken Mamyrbayev ^{1,†,‡} , Sergii Pavlov ^{2,‡}, Yosip Saldan ^{3,‡}, Kymbat Momynzhanova ^{4,‡} and Sholpan Zhumagulova ^{4,*}

¹ Institute of Information and Computational Technologies, Almaty, 050010, Kazakhstan; morkenj@mail.ru

² Vinnytsia National Technical University, Vinnytsia, 21000, Ukraine; psv@vntu.edu.ua

³ National Pirogov Memorial Medical University; ysaldan@ukr.net

⁴ Kazakh National University, Faculty of Information Technology, Almaty, 050038, Kazakhstan; kymbat010809@gmail.com

* Correspondence: kymbat010809@gmail.com; Tel.: (optional; include country code; if there are multiple corresponding authors, add author initials) +7 747 438 4488 (F.L.)

† Current address: Affiliation.

‡ These authors contributed equally to this work.

Abstract: For the first time, mathematical models were obtained for evaluating biomedical images using fuzzy set methods on the basis of expert knowledge bases, which made it possible to carry out complex qualitative diagnostics and increase the reliability and efficiency of diagnosis, to form a methodology for analyzing biomedical images based on the fuzzy set apparatus, which allowed to more fully assess the level of the disease for glaucoma. Aspects of practical implementation of the optical-electronic system of biomedical information processing are considered. An algorithm and an optical-electronic system of biomedical image analysis are proposed, which are used to increase the informativeness and reliability of diagnosing eye pathologies, in particular, glaucoma.

Keywords: optical and electronic expert system; diagnosing eye pathology; glaucoma

1. Introduction

When experts form a reference sample of images of the fundus, conflicting moments may arise due to the ambiguity of the images. Practice has shown that even one expert at different times (after a week, a month) can differently assess whether the same image belongs to glaucoma or not. It is natural that different experts often have different opinions about the attribution of fundus images to glaucoma. Therefore, when forming the knowledge base of the expert system, it is necessary to provide procedures for assessing the convergence and reproducibility of the results of creating a reference sample [1,2,3]. The result of the work of the optical-electronic expert system is a conclusion about the presence of glaucoma up to a certain type with an indication of the probability assessment. The latter will require the creation of the necessary volume of a representative reference sample of images [4,5,6]. A feature of the considered expert system is that, along with the knowledge of experts accumulated in it, a database is created based on the results of measuring quantitative features obtained as a result of automated image processing. Next, a conclusion is formed based on the assessment of the probability of the considered image belonging to the list of possible types of glaucoma [2,7,8,9]. Since the conclusion based on the results of drug research using an expert system is formed on the basis of the results of computer image processing, it is necessary to consider the factors affecting the accuracy of the measurements performed in the system [10, 12,13]. For the considered task of automating the analysis of the fundus, at the first stage, image improvement procedures are performed, which are associated with the suppression of image-distorting factors (filtering of obstacles, elimination of lighting irregularities, etc.). At the description stage, the features characteristic of the object are calculated, on the basis of which, at the third stage, the object is assigned to one or another class. The key of these three stages is the description stage. The recognition result depends on the choice of features and their informativeness (the ability to attribute the object to one or another class based on the value of the feature). We can distinguish two groups of factors that influence the recognition result: the first is the properties of the object itself (images of the fundus are very diverse); the second

is the image formation conditions (sensor noise, uneven illumination of the object, etc.) [14,15]. The purpose of this work is to develop a conceptual model of an optical-electronic expert system for the diagnosis of glaucoma using computer processing methods, as well as to analyze the influence of factors influencing the result of fundus image recognition [16,17,18].

2. Method

The proposed approach to the recognition of images of the fundus is based on the use of the knowledge of specialists in the field of ophthalmology and consists in creating an expert system for the diagnosis of glaucoma. The basis of the system is a reference sample of digital images, the description of which is stored in the knowledge base, an important component of the system is the analytical subsystem, which includes many rules by which decisions are made (Figure 1) [19,20,21]. Factors that have a dominant influence on the correctness of image recognition. As a result of the conducted research, a number of factors that have the most significant impact on the accuracy of the measurement results were identified, and they can be divided into three groups based on the type of source (Figure 2). For the considered system, instrumental factors can be classified into two groups: the first - factors due to physical processes in the used equipment; the second - factors due to the influence of external conditions. The first group of instrumental factors includes the noise of the image sensor, color distortions of the camera, brightness distortions, diffraction effects of the optical system, uneven spectral characteristics of the illuminator in the ophthalmoscope, uneven illumination of the drug in the field of view of the camera, etc. The factors of the second group include factors determined by the external conditions of system application [22,23,24].

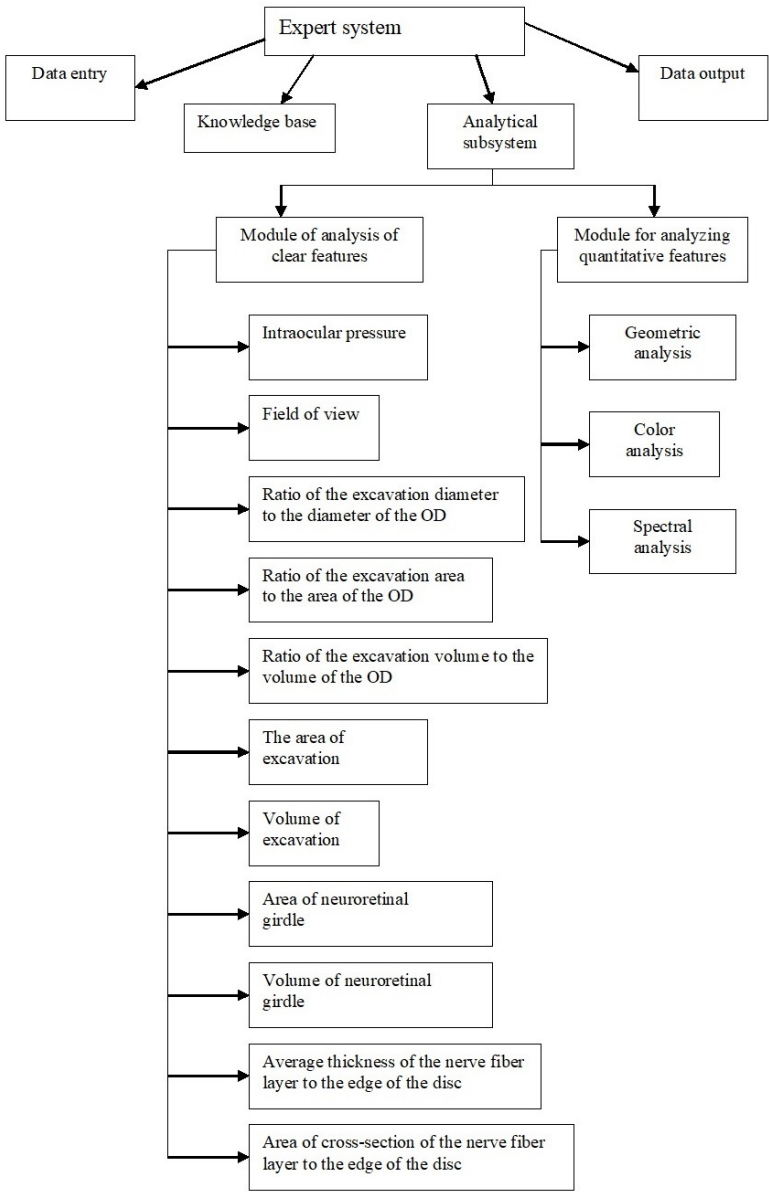


Figure 1. Analytical subsystem, which includes many rules, according to which decision-making is carried out.

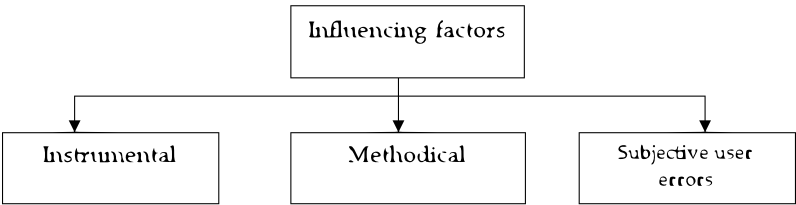


Figure 2. Factors that have the most significant impact on the accuracy of measurement results.

So, for example, the image registered in the system can be affected by such factors as the presence of bright external lighting (sunlight), as a result of which the contrast of the image can decrease. In addition, external factors include surface vibration (this can lead to image distortion at large exposures) [25,26]. First of all, methodical factors include the measurement model and mathematical methods of image processing, which are implemented in the system software, discretization and quantization operations when forming a digital image. A group of factors depending on the user is related to

the setting of the ophthalmoscope (choice of the lens, position of the condenser, field and aperture diaphragm, voltage of the lamp and light flux correction filters, position of the lens focus). Along with this, this group includes factors related to the selection of the field for research and positioning of the research object in the field of view of the camera, and factors that depend on the user in the interactive mode of image processing (when the processing parameters are specified by the user during the application software implementing image processing)[27-29]. A conceptual model of an expert system for diagnosing glaucoma is proposed, which will reduce the ambiguity of the interpretation of research objects. Factors affecting the correctness of recognition of complex objects (images of the fundus) using an expert system based on methods of computer ophthalmoscopy were considered (Table 1).

Table 1. Formation of an expert base in the diagnosis of glaucoma.

Severity of pathology	Intraocular pressure, mm Hg	Field of vision	Ratio of excavation diameter to OD diameter	Ratio of excavation area to OD area	Ratio of excavation volume to OD volume	Excavation area	Excavation volume	Area of the neuroretinal band	Volume of the neuroretinal girdle	Average thickness of the nerve fiber layer along the edge of the disc	Cross-sectional area of the nerve fiber layer along the edge of the disc
<i>d1 – normal</i>	15 – 21	60 ⁰	0,009~0,635	0~0,42	0~1,1	0~0,95	0~0,295	1,097~2,14	0,165~0,7	0,13~0,4	0,603~2,03
<i>d2~Istageofglaucoma</i>	15 – 21	50 ⁰	0,55~0,8	0,3~0,62	0,2~2,6	0,55~1,77	0,04~0,52	0,79~2,04	0,12~0,53	0,06~0,34	0,26~1,26
<i>d3~IIstageofglaucoma</i>	31	45 ⁰ – 35 ⁰	0,5~0,92	0,25~0,82	0,2 – 8	0,7~2,04	0,1~0,74	0,32~2,04	0,07~0,49	0,02~0,22	0,1~1,11
<i>d4~IIIstageofglaucoma</i>	33	< 35 ⁰	0,65~1,0	0,4~0,97	1,0 – 35	0,82~2,47	0,15~1,35	0,217~2,09	0,025~0,262	–0,12~0,26	–0,6~1,5

To diagnose glaucoma, we take into account the following indicators

X1 - Intraocular pressure, mm Hg.

X2 - Field of vision

X3 - The ratio of the diameter of the excavation to the diameter of the DZN

X4 - The ratio of the excavation area to the area of DZN

X5 - The ratio of the volume of excavation to the volume of DZN

X6 - Excavation area

X7 - Excavation volume

X8 - Neuroretinal strip area

X9 - Volume of the neuroretinal strip

X10 - The average thickness of the layer of nerve fibers along the edge of the disc

X11 - Cross-sectional area of the layer of nerve fibers along the edge of the disc.

For d_1 variable

$$\mu^{d_1}\left(\frac{x_1}{x_{11}}\right) = \mu^H(x_1) \cdot \mu^B(x_2) \cdot \mu^H(x_3) \cdot \mu^H(x_4) \cdot \mu^H(x_5) \cdot \mu^H(x_6) \cdot \mu^H(x_7) \cdot \mu^{BC}(x_8) \cdot \\ \cdot \mu^{HC}(x_9) \cdot \mu^C(x_{10}) \cdot \mu^C(x_{11}) \vee \mu^{HC}(x_1) \cdot \mu^B(x_2) \cdot \mu^{HC}(x_3) \cdot \mu^{HC}(x_4) \cdot \mu^H(x_5) \cdot \mu^{HC}(x_6) \cdot \mu^{HC}(x_7) \cdot \\ \mu^B(x_8) \cdot \mu^C(x_9) \cdot \mu^{BC}(x_{10}) \cdot \mu^{BC}(x_{11}) \vee \mu^{HC}(x_1) \cdot \mu^B(x_2) \cdot \mu^C(x_3) \cdot \mu^C(x_4) \cdot \mu^H(x_5) \cdot \mu^C(x_6) \cdot \mu^{HC}(x_7) \cdot \\ \mu^B(x_8) \cdot \mu^{BC}(x_9) \cdot \mu^B(x_{10}) \cdot \mu^B(x_{11}) \vee \mu^{HC}(x_1) \cdot \mu^B(x_2) \cdot \mu^{BC}(x_3) \cdot \mu^C(x_4) \cdot \mu^H(x_5) \cdot \mu^C(x_6) \cdot \mu^{HC}(x_7) \cdot \\ \mu^B(x_8) \cdot \mu^B(x_9) \cdot \mu^B(x_{10}) \cdot \mu^B(x_{11}) \vee \mu^{HC}(x_1) \cdot \mu^B(x_2) \cdot \mu^{BC}(x_3) \cdot \mu^C(x_4) \cdot \mu^H(x_5) \cdot \mu^C(x_6) \cdot \mu^{HC}(x_7) \cdot \\ \mu^B(x_8) \cdot \mu^B(x_9) \cdot \mu^B(x_{10}) \cdot \mu^B(x_{11})$$

For d_2 variable

$$\mu^{d_2}\left(\frac{x_1}{x_{11}}\right) = \mu^H(x_1) \cdot \mu^B(x_2) \cdot \mu^H(x_3) \cdot \mu^H(x_4) \cdot \mu^H(x_5) \cdot \mu^H(x_6) \cdot \mu^H(x_7) \cdot \mu^{BC}(x_8) \\ \cdot \mu^{HC}(x_9) \cdot \mu^C(x_{10}) \cdot \mu^C(x_{11}) \vee \mu^{HC}(x_1) \cdot \mu^B(x_2) \cdot \mu^{HC}(x_3) \cdot \mu^{HC}(x_4) \cdot \mu^H(x_5) \cdot \mu^{HC}(x_6) \\ \cdot \mu^{HC}(x_7) \cdot \mu^B(x_8) \cdot \mu^C(x_9) \cdot \mu^{BC}(x_{10}) \cdot \mu^{BC}(x_{11}) \vee \mu^{HC}(x_1) \cdot \mu^B(x_2) \cdot \mu^C(x_3) \cdot \mu^C(x_4) \cdot \mu^H(x_5) \cdot \mu^C(x_6) \cdot \\ \mu^{HC}(x_7) \cdot \mu^B(x_8) \cdot \mu^{BC}(x_9) \cdot \mu^B(x_{10}) \cdot \mu^B(x_{11}) \vee \mu^{HC}(x_1) \cdot \mu^B(x_2) \cdot \mu^{BC}(x_3) \cdot \mu^C(x_4) \cdot \mu^H(x_5) \cdot \mu^C(x_6) \cdot \\ \mu^{HC}(x_7) \cdot \mu^B(x_8) \cdot \mu^B(x_9) \cdot \mu^B(x_{10}) \cdot \mu^B(x_{11}) \vee \mu^{HC}(x_1) \cdot \mu^B(x_2) \cdot \mu^{BC}(x_3) \cdot \mu^C(x_4) \cdot \mu^H(x_5) \cdot \mu^C(x_6) \cdot \\ \mu^{HC}(x_7) \cdot \mu^B(x_8) \cdot \mu^B(x_9) \cdot \mu^B(x_{10}) \cdot \mu^B(x_{11})$$

For d_3 variable

$$\mu^{d_3}(x_1 \div x_{11}) = \mu^H(x_1) \cdot \mu^B(x_2) \cdot \mu^H(x_3) \cdot \mu^H(x_4) \cdot \mu^H(x_5) \cdot \mu^H(x_6) \cdot \mu^H(x_7) \cdot \mu^{BC}(x_8) \\ \cdot \mu^{HC}(x_9) \cdot \mu^C(x_{10}) \cdot \mu^C(x_{11}) \vee \mu^{HC}(x_1) \cdot \mu^B(x_2) \cdot \mu^{HC}(x_3) \cdot \mu^{HC}(x_4) \cdot \mu^H(x_5) \cdot \mu^{HC}(x_6) \cdot \mu^{HC}(x_7) \cdot \\ \mu^B(x_8) \cdot \mu^C(x_9) \cdot \mu^{BC}(x_{10}) \cdot \mu^{BC}(x_{11}) \vee \mu^{HC}(x_1) \cdot \mu^B(x_2) \cdot \mu^C(x_3) \cdot \mu^C(x_4) \cdot \mu^H(x_5) \cdot \mu^C(x_6) \cdot \mu^{HC}(x_7) \cdot \mu^B(x_8) \cdot \mu^{BC}(x_9) \cdot \mu^B(x_{10}) \cdot \mu^B(x_{11}) \vee \\ \mu^{HC}(x_1) \cdot \mu^B(x_2) \cdot \mu^{BC}(x_3) \cdot \mu^C(x_4) \cdot \mu^H(x_5) \cdot \mu^C(x_6) \cdot \mu^{HC}(x_7) \cdot \mu^B(x_8) \cdot \mu^B(x_9) \cdot \mu^B(x_{10}) \cdot \mu^B(x_{11}) \vee \\ \mu^{HC}(x_1) \cdot \mu^B(x_2) \cdot \mu^{BC}(x_3) \cdot \mu^C(x_4) \cdot \mu^H(x_5) \cdot \mu^C(x_6) \cdot \mu^{HC}(x_7) \cdot \mu^B(x_8) \cdot \mu^B(x_9) \cdot \mu^B(x_{10}) \cdot \mu^B(x_{11})$$

For d_4 variable

$$\mu^{d_4}\left(\frac{x_1}{x_{11}}\right) = \mu^H(x_1) \cdot \mu^B(x_2) \cdot \mu^H(x_3) \cdot \mu^H(x_4) \cdot \mu^H(x_5) \cdot \mu^H(x_6) \cdot \mu^H(x_7) \cdot \mu^{BC}(x_8) \\ \cdot \mu^{HC}(x_9) \cdot \mu^C(x_{10}) \cdot \mu^C(x_{11}) \vee \mu^{HC}(x_1) \cdot \mu^B(x_2) \cdot \mu^{HC}(x_3) \cdot \mu^{HC}(x_4) \cdot \mu^H(x_5) \cdot \mu^{HC}(x_6) \\ \cdot \mu^{HC}(x_7) \cdot \mu^B(x_8) \cdot \mu^C(x_9) \cdot \mu^{BC}(x_{10}) \cdot \mu^{BC}(x_{11}) \vee \mu^{HC}(x_1) \cdot \mu^B(x_2) \cdot \mu^C(x_3) \cdot \mu^C(x_4) \cdot \mu^H(x_5) \cdot \mu^C(x_6) \cdot$$

$$\mu^{HC}(x_7) \cdot \mu^B(x_8) \cdot \mu^{BC}(x_9) \cdot \mu^B(x_{10}) \cdot \mu^B(x_{11}) \vee$$
$$\mu^{HC}(x_1) \cdot \mu^B(x_2) \cdot \mu^{BC}(x_3) \cdot \mu^C(x_4) \cdot \mu^H(x_5) \cdot \mu^C(x_6) \cdot \mu^{HC}(x_7) \cdot \mu^B(x_8) \cdot \mu^B(x_9) \cdot \mu^B(x_{10}) \cdot \mu^B(x_{11}) \vee$$
$$\mu^{HC}(x_1) \cdot \mu^B(x_2) \cdot \mu^{BC}(x_3) \cdot \mu^C(x_4) \cdot \mu^H(x_5) \cdot \mu^C(x_6) \cdot \mu^{HC}(x_7) \cdot \mu^B(x_8) \cdot \mu^B(x_9) \cdot \mu^B(x_{10}) \cdot \mu^B(x_{11}).$$

3. Software-Algorithmic Implementation for Processing Biomedical Images

During the analysis of the characteristics of the fundus, increase the reliability of the final assessment of fundus images by using expert methods. The proposed approach to the recognition of images of the fundus is based on the use of the knowledge of specialists in the field of ophthalmology and consists in creating an expert system for the diagnosis of glaucoma. The basis of the system is a reference sample of digital images, the description of which is stored in the knowledge base, an important component of the system is the analytical subsystem, which includes many rules by which decisions are made. To obtain a diagnosis with the help of an expert database, we suggest using elements of fuzzy logic. We will build the model on the basis of actual data. (Table 1). Using the algorithm of the processing method based on the fuzzy logic apparatus, we get:



Figure 3. Initial data input request.

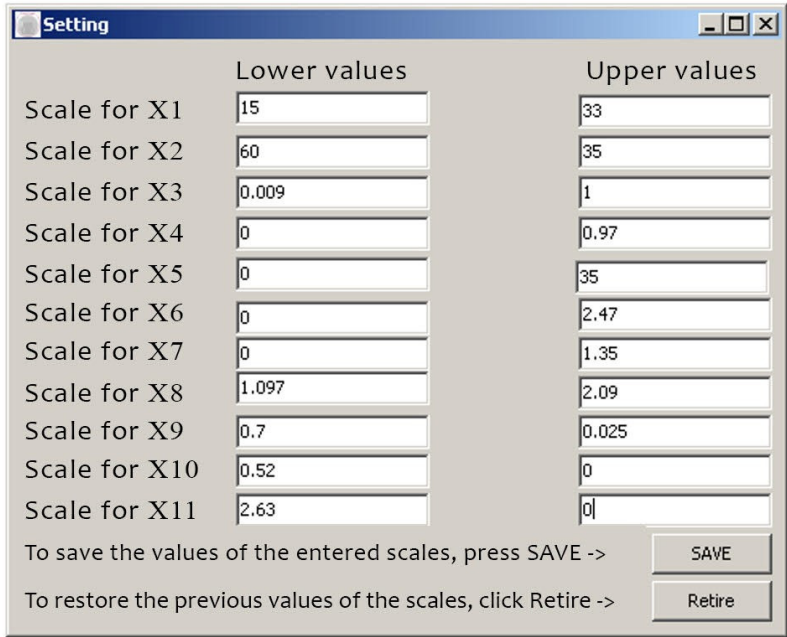


Figure 4. Input of initial data.

When saving the data, i.e. entering the lower and upper values, we can enter the patient’s data:

Figure 5. Entering the patient's input data .

Having obtained the result, we can conclude that the patient has glaucoma of the 3rd degree.

4. Physical Modeling of the Optical-Electronic System for Researching Pathologies of the Fundus

The optical-electronic system for obtaining an image of the retina of the eye refers to medicine, namely to devices for examining the fundus, and can be used in ophthalmology to conduct medical and biological research, namely: to fix the image of the retina. At the same time, the optical channel is realized as follows. The radiation flow coming from the radiating surface of the source to the remote illuminating surface (1):

$$\Phi = L \cdot S_{source} \cdot S_{sq} \cdot \frac{(\cos \beta_1 \cdot \cos \beta_2)}{l^2} \quad (1)$$

where L is the brightness of the emitting surface;

S source – the area of the radiating surface;

S sq. is the area of the illuminating surface;

β_1 is the angle between the direction of radiation propagation and the normal to the radiating surface;

β_2 is the angle between the direction of radiation propagation and the normal to the illuminating surface;

l is the distance between the surfaces.

If the lighting system directs radiation into the eye through a pupil area with an area Ssource, then this area can be considered as a light-emitting surface, the brightness of which L_{laser} due to the transition of light rays from the air to the eye is related to the brightness of the source - the LED Ldiode by the expression (1, 2) :

$$L_{laser} = n_{eye}^2 \cdot L_{diode} \quad (2)$$

N_{eye} – is the average refractive index of eye tissues. Taking into account expression (2) and the transmission coefficient of the optical system of the eye τ_{eye} , expression (1) for the light flux falling on the retina will be written in the form:

$$F = \tau_{eye} \cdot n_{eye}^2 \cdot L_{diode} \cdot S'_{source} \cdot S_{eye'} \cdot \frac{(\cos \beta_1 \cdot \cos \beta_2)}{l_{eye}^2}, \quad (3)$$

where $S_{eye'}$ is the area of the retina; l_{eye} is the distance between the pupil and the retina.

When the light flux spreads along the optical axis of the eye, which is assumed to be perpendicular to the planes of the pupil and retina ($\beta_1 = \beta_2 = 0$), the illumination of the retina will be:

$$E_{oka} = \frac{F}{S_{sq}} = \frac{\tau_{eye} \cdot n_{eye}^2 \cdot L_{diode} \cdot S'_{source}}{l_{eye}^2} \tag{4}$$

Expression (4) is true for the illumination of a retinal point lying on the optical axis of the eye. However, since the fundus is a sphere and due to the multiple reflection of light rays inside the eye, it can be assumed that the illumination of the entire retina is uniform and is determined by expression (4). A uniformly illuminated retina, diffusely reflecting the light stream falling on it, represents a secondary light source, the brightness of which will be equal to:

$$L_{eye} = \frac{\rho \cdot E_{eye}}{\pi} = \frac{\rho \cdot \tau_{eye} \cdot n_{eye}^2 \cdot L_{diode} \cdot S'_{source}}{\pi \cdot l_{eye}^2}, \tag{5}$$

where ρ is the diffusion reflection coefficient.
Illumination of the retinal image on the photomatrix, which is built by the optical system:

$$E' = \frac{\tau_{os} \cdot \pi \cdot L_c}{4} \cdot \left(\frac{n'}{n}\right)^2 \cdot \left(\frac{D}{f'}\right)^2 \cdot \frac{\beta_p^2}{(\beta_p - \beta)^2}, \tag{6}$$

where τ_{os} is the transmission coefficient of the optical system;
 n' is the refractive index of the medium in the image space $n' = 1$;
 n is the index of refraction of the medium in the space of objects ($n = n_{oka}$);
 D is the diameter of the entrance pupil of the optical system;
 f' is the focal length of the optical system;
 β_p – linear increase of the optical system in the pupils;
 β is the linear increase of the optical system.

Substituting (5) into (6) and assuming a linear increase in the pupils $\beta_p = 1$, for the illumination of the retinal image on the photo matrix we obtain:

$$E' = \frac{\tau_{oc} \cdot \tau_{oka} \cdot \rho \cdot L_{cd} \cdot S'_{dj}}{4 \cdot l_{oka}^2} \cdot \left(\frac{D}{f'}\right)^2 \cdot \frac{1}{(1 - \beta)^2}, \tag{7}$$

Let's assume that $\tau_{eye} = 0,5$; $\tau_{os} = 0,9$; $\rho = 0,2$; $l_{eye} = 24$ diameter = 24 mm. The maximum brightness of the light source that can be transmitted when directly observed is $7500 \frac{cd}{m^2}$. For so that the patient does not feel discomfort, as an illuminator we choose an LED for which $Lsd = 7000 \frac{cd}{m^2}$. Let's also assume that the projection of the source onto the pupil of the eye occupies 50% of its area. In this case, with a pupil diameter of 6 mm, $Sd.pup = 14.13$ mm. To perceive the image, we will use the 6.6 Megapixel CMOS photo matrix NOII4SM6600A, the main indicators of which are as follows:

Table 2. Formation of an expert base in the diagnosis of glaucoma.

Dimensional capacity	2210 × 3002	¹ Tables may have a footer.
Optical format, inch	1	
Range of spectral sensitivity, nm	400...1000	
Apparent sensitivity, $\frac{V}{s}$	2.01	
Dark signal, $\frac{mV}{s}$	3.37	

The required linear increase β of the optical system can be determined by the ratio that corresponds to the condition under which the retinal image occupies the largest part of the photomatrix area:

$$\beta = \frac{H_{phm}}{D_c} \quad (8)$$

where H_{phm} is the height of the photomatrix;
Dretina is the diameter of the retina.

The optical matrix format of 1 inch corresponds to the size of 12.8×9.6 mm. The diameter of the human retina is 22 mm. Then

$$\beta = \frac{9.6}{22} = 0.436. \quad (9)$$

By substituting numerical values for the definition in expression (7), we get:

$$E' = \frac{0,9 \cdot 0,5 \cdot 0,2 \cdot 7000 \cdot 14,13}{4 \cdot 24^2} \cdot \left(\frac{D}{f'}\right)^2 \cdot \frac{1}{(1 - 0.436)^2} = 12.146 \cdot \left(\frac{D}{f'}\right)^2, \quad (10)$$

To carry out further calculations, we will determine the illumination of the photomatrix E' , at which the value of the useful output signal will be comparable to the dark one. The minimum illumination of the image, at which it is indistinguishable from the background noise, is found using the sensitivity of the photomatrix and the value of the dark signal:

$$E_0 = \frac{3.37 \cdot 10^{-3}}{2.01} = 1.677 \cdot 10^{-3} (Lx)$$

To obtain a good image of the retina, the illumination of the photo matrix must be at least 10 times higher than this value, therefore:

$$E' = 0.01677 (Lx)$$

Then, from expression (9) for the geometric luminous intensity of the optical system, we have:
 $\left(\frac{D}{f'}\right)^2 = \frac{0.01677}{12.146} = 1.38 \cdot 10^{-3}$ In order to use the entire field of the optical system, its entrance pupil must be aligned with the plane of the eye pupil. In this case, the field aperture will be the frame of the photomatrix, and with the linear magnification selected in accordance with expression (8), the image of the entire retina will be formed on the photomatrix. The diameter of the entrance pupil of the optical system D is chosen equal to 3 mm. As a result, the area of the entrance pupil of the optical system will be equal to 7.065 mm^2 , which is 25% of the area of the pupil of the eye with a pupil diameter of 6 mm. Then, from expression (10) for the focal length of the optical system, we obtain:

$$f' = \frac{9}{1.38 \cdot 10^{-3}} = 80.76 (mm)$$

When calculating the focal length of the optical system, its linear increase in the pupils β_p was taken to be equal to 1. This corresponds to the case when the distance $-z_p$ from the front focus of the optical system to the input pupil is equal to the front focal length of the optical system:

$$-z_p = -f = -80.76$$

(mm)

The distance from the front focus to the retina will be equal to:

$$-z = -z_p - l_{oka} = -80.76 - 24 = -104.76$$

(mm) The distance z' from the back focus to the retinal image formed in the photomatrix plane is determined using the linear magnification of the optical system β :

$$z' = \beta \cdot f' = 0.436 \cdot 80.76 = 35.21(mm)$$

5. Evaluation of Metrological Indicators

For most medical and biological studies, the degree of probability of an error-free forecast equal to 95% is considered sufficient, and the number of cases of the general population in which deviations from the patterns established during a sample study may be observed will not exceed 5%. In a number of studies related, for example, to the use of highly toxic substances, vaccines, surgical treatment, etc., as a result of which serious diseases, complications, and fatal consequences are possible, the degree of probability $P = 99.7\%$ is used, i.e. no more than in 1% of cases of the general population, deviations from the regularities established in the sample population are possible. The given degree of probability (P) of an error-free forecast corresponds to a certain, substituted into the formula, value of the criterion t , which also depends on the number of observations. When $n > 30$, the degree of probability of an error-free forecast $P = 99.7\%$ corresponds to the value of $t = 3$, and when $P = 95.5\%$ - the value of $t = 2$. When $n < 30$, the value of t at the appropriate degree of probability of an error-free forecast is determined according to a special table (N.A. Plokhinsky). We will determine the error of representativeness (mp) and confidence limits of the relative indicator of the general population (R_{gen}) in relation to the table of results obtained by the diagnosis of an ophthalmologist and with the help of an expert database. A group of glaucoma patients consisting of 42 people aged 50-65 years, but with different stages, was taken.

Table 2 - Comparison of the received diagnoses by different methods

Table 3. Formation of an expert base in the diagnosis of glaucoma.

Dimensional capacity	Stages of glaucoma	Number of patients in percent	Number of patients	Stages of glaucoma	Number of patients in percent
18	I	43	17	I	40
6	II	14	5	II	12
18	III	43	20	III	48

¹ Tables may have a footer.

Determination of the representativeness error of the relative indicator according to the diagnosis of the ophthalmologist:

$$m_{1b} = \sqrt{\frac{43 \times (100 - 43)}{42}} = 7.64\%$$
$$m_{2b} = \sqrt{\frac{14 \times (100 - 43)}{42}} = 5,35\%$$
$$m_{3b} = \sqrt{\frac{43 \times (100 - 43)}{42}} = 7.64\%$$

Determination of the error of representativeness of the relative indicator according to the diagnosis obtained with the help of the expert database:

$$m_{1c} = \sqrt{\frac{40 \times (100 - 40)}{42}} = 7.56\%$$
$$m_{2c} = \sqrt{\frac{12 \times (100 - 12)}{42}} = 5,01\%$$

$$m_{3c} = \sqrt{\frac{48 \times (100 - 48)}{42}} = 7.71\%$$

The confidence limits of the average value of the general population (R_{gen}) are calculated as follows:

- it is necessary to set the degree of probability of an error-free forecast ($P = 95\%$);
- at a given degree of probability and the number of observations is more than 30, the value of the criterion t is equal to 2 ($t = 2$). Then $P_{1b} = P_{choice} \pm tm = 43\% \pm 2 \times 7,64 = 43\% \pm 15,28\%$

Then $P_{2b} = P_{choice} \pm tm = 14\% \pm 2 \times 5,35 = 14\% \pm 10,70\%$

Then $P_{3b} = P_{choice} \pm tm = 43\% \pm 2 \times 7,64 = 43\% \pm 15,28\%$

Then $P_{1c} = P_{choice} \pm tm = 40\% \pm 2 \times 7,56 = 40\% \pm 15,12\%$

Then $P_{2c} = P_{choice} \pm tm = 12\% \pm 2 \times 5,01 = 12\% \pm 10,02\%$

Then $P_{3c} = P_{choice} \pm tm = 48\% \pm 2 \times 7,71 = 48\% \pm 15,42\%$

Taking into account the results of the calculation of the confidence limits of the average value of the general population (R_{gen}), we can establish with the probability of an error-free forecast $P = 95\%$ that the frequency of detection of stage I glaucoma at the age of 50-65 will be in the range from 27.72 % to 58, 28 % of cases (diagnosis by an ophthalmologist) and from 24.88 % to 55.12 % (diagnosis obtained using an expert database). The frequency of detection of stage II glaucoma at the age of 50-65 years will range from 3.30 % to 24.70 % of cases (diagnosis by an ophthalmologist) and from 1.98 % to 22.02 % (diagnosis obtained by expert base). The frequency of detection of stage III glaucoma at the age of 50-65 years will range from 27.72 % to 58.28 % of cases (diagnosis by an ophthalmologist) and from 32.58 % to 63.42 % (diagnosis obtained by expert base).

6. Recommendations for the Implementation of the Optic-Electronic System for Obtaining an Image of the Retina of the Eye

In Figure 6 shows a schematic representation of the path of the rays in the design of the photographic ophthalmoscope, which is designed to fix the image of the retina, in Figure 7 presents an optical-electronic system for the analysis of ophthalmological images, in Figure 8 – the image of the retina of the human eye, which was obtained as a result of using a photographic ophthalmoscope, is presented.

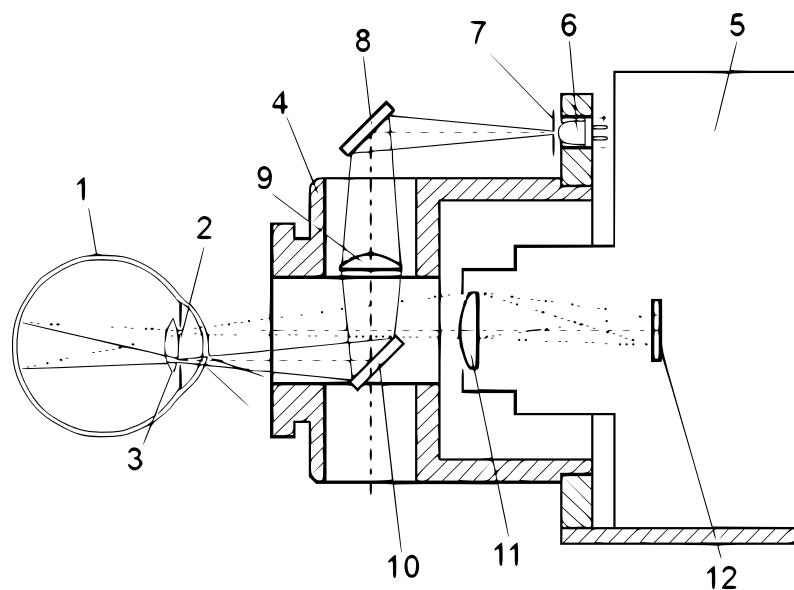


Figure 6. This is a figure. Schemes follow the same formatting. If there are multiple panels, they should be listed as: (a) Description of what is contained in the first panel. (b) Description of what is contained in the second panel. Figures should be placed in the main text near to the first time they are cited. A caption on a single line should be centered.

Photographic ophthalmoscope, the body of the optical nozzle 4, in which the optical system containing the diaphragm 7, the first 8, the second 10 mirrors and the condenser 9 is located. In addition, the device contains a digital camera 5, a white LED 6, a digital camera lens 11, a matrix digital camera 12, as well as in Figure 6 shows the location of the patient's eye 1, its pupil 2 and its lens 3, and the patient's eye 1, which has a pupil 2 and a lens 3, is connected to the output of the second mirror 10, the input of which is connected to the input of the condenser 9 and the lens of the digital camera 11, the output of which is connected to the input of the matrix of the digital camera 12, the output of the condenser 9 is connected to the first mirror 8, the input of which is connected to the diaphragm 7, which is connected to the output of the white LED 6 [30-32]. The photographic ophthalmoscope works as follows. Scattered light from the white LED 6, through the aperture 7 is focused by the system of mirrors 8, 10 and the condenser 9, passing through the pupil 2 and the lens 3 of the eye 1, illuminates the fundus. The optical system, which consists of the diaphragm 7, mirrors 8 and 10 and the condenser 9, is placed in the body of the optical nozzle 4. The image of the fundus passes through the optical system of the eye 1 and in a parallel beam hits the lens of the digital camera 11 contained in the digital camera 5, where an enlarged image of the retina is formed (Figure 4.4), which is displayed using a digital matrix 12 for further analysis by a doctor. Due to the introduction of a white LED, mirrors, condenser, lens and matrix of a digital camera, the functionality of the ophthalmoscope was increased, which gives the doctor the opportunity to improve the diagnosis of eye diseases and to be able to reproduce the medical history.



Figure 7. Optical-electronic system for the analysis of ophthalmic images.

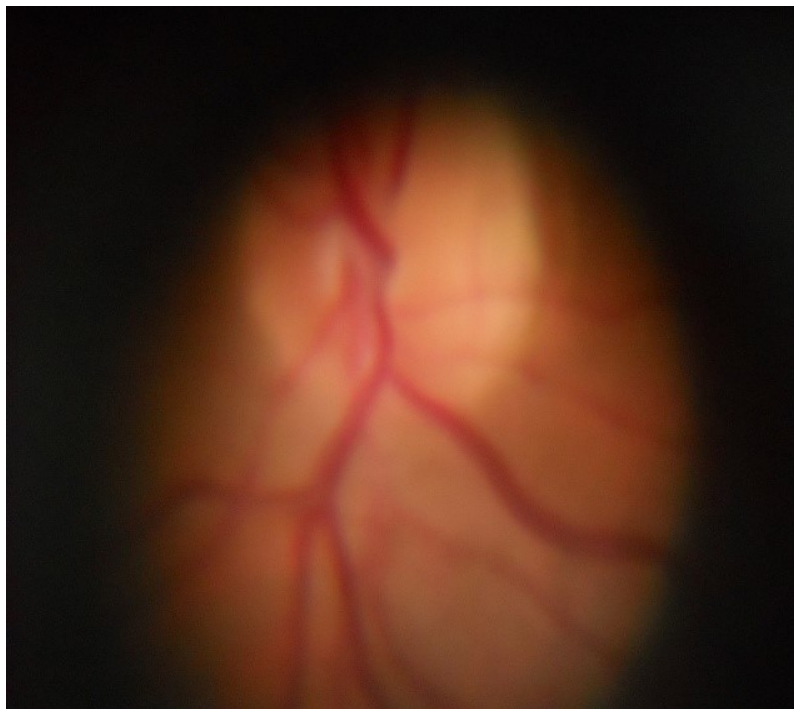


Figure 8. Image of the retina.

7. Conclusions

For the first time, mathematical models were obtained for evaluating biomedical images using fuzzy set methods on the basis of expert knowledge bases, which made it possible to carry out complex qualitative diagnostics and increase the reliability and efficiency of diagnosis, to form a methodology for analyzing biomedical images based on the fuzzy set apparatus, which allowed to more fully assess the level of the disease for glaucoma. Aspects of practical implementation of the optical-electronic system of biomedical information processing are considered. An algorithm and an optical-electronic system of biomedical image analysis are proposed, which are used to increase the informativeness and reliability of diagnosing eye pathologies, in particular, glaucoma. On the basis of the developed model and algorithms, a hardware and software implementation was created, experimental and medical studies of the obtained system indicators were conducted. Examples of practical application of the developed optical-electronic system for the analysis of eye pathologies are given. The main practical result is that the expediency and reliability of such an optical-electronic system has been practically confirmed.

Acknowledgments: This research has been funded by the Committee of Science of the Ministry of Science and Higher Education of the Republic of Kazakhstan (Grant No. AP 19675574).

Conflicts of Interest: The authors declare no conflicts of interest.

References

1. Sebestyen G.S., Decision Making Processes in Pattern Recognition. N.Y.: Macmillan **1995**, 10, 237 p.
2. Fukushima K. Neural Network for Visual Pattern Recognition. In *Comput*; **1988**, 21, pp. 65–116.
3. Dogru M., Katakami Ch., Inoue M., Ocular microcirculation changes in noninsulin-dependent diabetes mellitus. *Ophthalmology* **2001**, V. 108. - № 3., pp. 586-592.
4. Novotny H., Alvis D. A method of photographing fluorescence in circulating blood in the human retina. *Circulation* **1961**, V. 24. - № 7., pp.82-86.
5. Federman J., Brown G., Felberg N., Felton S. Experimental ocular angiogenesis *American Journal of Ophthalmology* **1980**, 10, pp.231-237.
6. Balashevich I., Izmailov A., Levochkin A. Diagnostic possibilities of digital fluorescein angiography *Ophthalmosurgery* **1998**, pp.38-46.

7. Crittin M., Schmidt H., Riva E. C. Hemoglobin oxygen saturation in the human ocular fundus measured by reflectance oximetry: preliminary data in retinal veins. *Klin. Monatsbl Augenheilkd* **2002**, 1, pp. 289-291.
8. Rotshtein A. Design and Tuning of Fussy IF – THEN Vuly for Medical Didicol Diagnosis. In Fussy and Neuro-Fussy Systems in Medicine (Eds: N. Teodovescu, A. Kandel, I. Lain.).USA. CRC-Press **1998**, 1, pp. 235–295.
9. Bardenheier BH, Lin J, Zhuo X, et al., Centers for Disease Control and Prevention. *National Diabetes Statistics Report Accessed* **2022**.
10. Murchison A.P, Hark L, Pizzi LT, et al., Non-adherence to eye care in people with diabetes.*BMJ Open Diabetes Res Care* **2017**, 5(1), pp. 235–295.
11. Vuytsyk V., Gotra O.Z., and Grigoryev V.V., "Expert systems: a training manual," *Lviv, Ukraine: Liga-Press* **2006**.
12. Zavhorodnia N. G., Sarzhevska L. E., Ivakhnenko O. M. etc. "Eye changes in general diseases of the body: education - method. *manual for intern doctors in the specialty "Ophthalmology", Zaporizhzhia*, 83, **2020**.
13. Brownlee, J., "Machine Learning Mastery with Python: Understand Your Data, Create Accurate Models and Work Projects End-to-End," 2nd Edition, California: Machine Learning Mastery (2019).
14. Lu, W. et al., "Application of computer-aided diagnosis in diabetic retinopathy screening: A review," *Computers in Biology and Medicine*, Vol. 103, 337-349 (2018).
15. Ting, D. et al., "Deep learning in ophthalmology: The technical and clinical considerations," *Progress in Retinal and Eye Research*, Vol. 72, 100759 (2019).
16. Abràmoff, M.D. et al. "Automated analysis of retinal images for detection of referable diabetic retinopathy," *JAMA Ophthalmology*, Vol. 131, 3, 351-357 (2013).
17. Roychowdhury, S. et al., "Automatic detection of diabetic retinopathy using deep learning," *International Conference on Computing, Analytics and Security Trends (CAST)*, 264-271 (2017).
18. Rupert R. A. Bourne, Gretchen A. Stevens, Richard A. White, etc., "Causes of vision loss worldwide, 1990–2010: a systematic analysis," *The Lancet Global Health*, Vol. 1, Issue 6, e339-e349 (2013).
19. Chakrabarti, Rahul, C. Alex Harper, and Jill Elizabeth Keeffe., "Diabetic retinopathy management guidelines," *Expert review of ophthalmology*, 7.5: 417-439 (2012).
20. Pavlov S. V., Karas O. V., and Sholota V. V., "Processing and analysis of images in the multifunctional classification laser polarimetry system of biological objects," *Proc. SPIE* 10750, pp. 107500N (Sept., 2018).
21. Pavlov S.V., Martianova T.A., Saldan Y.R., etc., "Methods and computer tools for identifying diabetes-induced fundus pathology", *Information Technology in Medical Diagnostics II*. CRC Press, Balkema book, Taylor and Francis Group, London, UK, 87-99, 2019.
22. SaldanYosyp, Sergii Pavlov, Vovkotrub Dina, Waldemar Wójcik, and etc., "Efficiency of optical-electronic systems: methods application for the analysis of structural changes in the process of eye grounds diagnosis," *Proc. SPIE* 10445, *Photonics Applications in Astronomy, Communications, Industry, and High Energy Physics Experiments 2017*, 104450S (2017).
23. Lytyvnenko, V., Lurie, I., Voronenko, M., etc., "The use of Bayesian methods in the task of localizing the narcotic substances distribution," *International Scientific and Technical Conference on Computer Sciences and Information Technologies*, 2, 8929835, 60–63 (2019).
24. Friedman, Jerome, Trevor Hastie, and Robert Tibshirani., "The elements of statistical learning," *hastie.su.domains/ElemStatLearn* (2009).
25. Kvyetnyy Roman, Bunyak Yuriy, Sofina Olga, and etc., "Blur recognition using second fundamental form of image surface," *Proc. SPIE* 9816, *Optical Fibers and Their Applications 2015*, 98161A (17 December 2015).
26. Avrunin O.G., Tymkovych M.Y., Saed H.F.I., etc., "Application of 3D printing technologies in building patient-specific training systems for computing planning in rhinology," *Information Technology in Medical Diagnostics II - Proceedings of the International Scientific Internet Conference on Computer Graphics and Image Processing and 48th International Scientific and Practical Conference on Application of Lasers in Medicine and Biology*, 7 (2019).
27. Mamyrbayev, O., Pavlov, S., Karas, O., Saldan, I., Momynzhanova, K., Zhumagulova, S. (2024). Increasing the reliability of diagnosis of diabetic retinopathy based on machine learning. *Eastern-European Journal of Enterprise Technologies*, 2 (9 (128)), 17–26. <https://doi.org/10.15587/1729-4061.2024.297849>
28. Abdiakhmetova Z.M. Wavelet data processing in the problems of allocation in recovery well logging *Journal of Theoretical and Applied Information Technology* 15th March 2017. Vol.95. No 5

29. Rysbek Baimakhan, Zhanar Kadirova, Assima Seinassinova, Aigerim Baimakhan, Zukhra Abdiakhmetova Mathematical Modeling of the Water Saturation Algorithm of the Mountain Slope on the Example of the Catastrophic Landslide of the Northern Tien Shan Ak Kain Mathematical Modelling of Engineering Problems Vol. 8, No. 3, June, 2021, pp. 467-476. URL:
32. Temirbekova, Z., Pyrkova, A., Z. M. Abdiakhmetova, Berdaly, A. Library of Fully Homomorphic Encryption on a Microcontroller SIST 2022 - 2022 International Conference on Smart Information Systems and Technologies, Proceedings, 2022 <https://doi.org/10.1109/SIST54437.2022.9945722>
32. Z. M. Abdiakhmetova, Berdaly, A., Temirbekova, Zh. Comparative Machine-Learning Approach: Study for Heart Diseases SIST 2022 - 2022 International Conference on Smart Information Systems and Technologies, Proceedings, 2022 <https://doi.org/10.26577/JMMCS.2022.v115.i3.10>
32. Fariza Nussipova, Shynggys Rysbekov, Zukhra Abdiakhmetova, Amandyk Kartbayev Optimizing loss functions for improved energy demand prediction in smart power grids International Journal of Electrical and Computer Engineering (IJECE) Vol. 14, No. 3, June 2024, pp. 3415 3426 ISSN: 2088-8708, DOI: 10.11591/ijece.v14i3.pp3415-3426.

Disclaimer/Publisher's Note: The statements, opinions and data contained in all publications are solely those of the individual author(s) and contributor(s) and not of MDPI and/or the editor(s). MDPI and/or the editor(s) disclaim responsibility for any injury to people or property resulting from any ideas, methods, instructions or products referred to in the content.